

# Recurrence analysis of strange nonchaotic dynamics

E. J. Ngamga<sup>1</sup>, A. Nandi<sup>2</sup>, R. Ramaswamy<sup>2</sup>, M. C. Romano<sup>1</sup>, M. Thiel<sup>1</sup>, J. Kurths<sup>1</sup>

<sup>1</sup>*Nonlinear Dynamics Group, Institute of Physics,*

*University of Potsdam, Potsdam 14415, Germany and*

<sup>2</sup>*School of Physical Sciences, Jawaharlal Nehru University, New Delhi 110 067, India*

(Dated: December 6, 2006)

We present new methods to detect the transitions from quasiperiodic to chaotic motion via strange nonchaotic attractors (SNAs). These procedures are based on the time needed by the system to recur to a previously visited state, and on a measure of the predictability in the system. The applicability of these techniques is demonstrated by detecting the transition to SNAs or the transition from SNAs to chaos in representative quasiperiodically forced discrete maps. The fractalization transition to SNAs—for which most existing diagnostics are inadequate—is clearly detected by recurrence analysis. These methods are robust to additive noise, and thus can be used in analyzing experimental time-series.

PACS numbers: 82.40.Bj, 83.85.Ns

## I. INTRODUCTION

Starting with the seminal works of Landau [1] and Ruelle and Takens [2], the transition from regular to chaotic dynamics via quasiperiodicity has attracted great interest. Different aspects of this transition have been studied both theoretically and experimentally over the past several decades. About two decades ago, however, it was found that in quasiperiodically forced systems the transition to chaos is generally mediated by strange nonchaotic attractors (SNAs). SNAs were first described by Grebogi *et al.* in 1984 [3] and since then have been investigated in a number of numerical [4–14], experimental [15, 16] and mathematical [17–20] studies. These unusual attractors are thought to be important for biological systems [10, 21] and for nonlinear dynamics based communication [22, 23].

SNAs are geometrically strange (or fractal) while they are nonchaotic in the dynamical sense. These attractors can be regarded as structures intermediate between regularity and chaos, since they possess properties which can be related either to regular or to chaotic processes. Typical trajectories experience arbitrarily long time intervals of expansion while on the average, contraction dominates. This behaviour yields a strange geometric structure in the phase space similar to those for chaotic attractors. Different routes to SNAs have been reported: (i) collision between a period-doubled torus and its unstable parent [7], (ii) fractalization of a torus [12], (iii) blowout bifurcation [24], and (iv) intermittency [13]. Most studies on SNAs have focused on their characterization using tools such as Lyapunov exponents and their variance, spectral properties [4, 5], geometrical properties [6, 10], local divergence of trajectory [25], phase sensitivity and rational approximations [8], functional maps and invariant curves [12, 26], as well as a renormalization-group analysis [27].

In the present work, we propose measures of complexity which are based on the *recurrences* of states in the phase space to detect transitions from regular to chaotic motion via SNAs. Moreover, they enable us to identify the strange nonchaotic behavior for the fractalization route to SNAs, which is not always apparent in measures based on the Lyapunov exponents. We further show that recurrence based measures are robust to additive noise, and are therefore highly suitable for the analysis of experiments [28] where the data may be both noisy and sparse.

The paper is organised as follows. In Section II, the recurrence measures that we use here are defined, and applied in Section III to the detection of some routes to SNAs in discrete 1-dimensional nonlinear mappings. Section IV examines the fractalization of a torus to an SNA, and Section V the transition from SNAs to chaos. The final section summarizes our results.

## II. MEASURES OF COMPLEXITY

The concept of recurrences in dynamical systems goes back to Poincaré [29], who showed that under certain conditions, the orbit of a bounded dynamical system must return arbitrarily close to each former point of its route with probability one. The time of return can, however, be arbitrarily long. A visual representation of such recurrences is provided by recurrence plots (RPs), which were introduced in 1987 [30]. RPs are defined for a given trajectory  $\{\mathbf{x}_i\}_{i=1}^N$ , of a dynamical system, where  $\mathbf{x}_i \in \mathbb{R}^n$ . They are based on the matrix

$$R_{i,j}^{(\delta)} = \Theta(\delta - \|\mathbf{x}_i - \mathbf{x}_j\|), \quad i, j = 1, \dots, N \quad (1)$$

where  $\delta$  is a predefined threshold,  $\Theta(\cdot)$  the Heaviside function and  $\|\cdot\|$  a norm (here the maximum norm). Close or  $\delta$ -recurrent points give “1” and separate points “0”. Then the values 1 and 0 are depicted as black and white dot in a two-dimensional plot, providing a visual representation of the system dynamics.

Special attention has to be paid to the choice of the threshold  $\delta$ . It is desirable that the smallest threshold possible is chosen. However the influence of noise can need a larger threshold, because noise would distort any existing structure in the RP. It has been suggested that this threshold should range from a few per cent of the maximum phase space diameter [31] and should not exceed 10% of the mean [32]. In the presence of observational noise, the choice  $\delta = 5\sigma$ , with  $\sigma$  being the standard deviation of the observational noise, has been shown to be more appropriate [33]. We use this latter choice.

Several measures have been proposed to quantify the structures in RPs, and have found applications in the analysis of physiological or geophysical time series [34–36]. It has been shown that all topological information about the underlying system is contained in the RP [37]. Gao [38] has introduced a recurrence time statistics that corresponds to vertical structures in the RPs. These statistics seem to be of special importance in the present study, since they are able to extract the information dimension of chaotic attractors, to detect nonstationarity of time series and to locate bifurcations and others types of changes in the dynamics. Marwan *et al.* [39] have proposed further measures of complexity to quantify vertical black structures in RPs: this permits the identification of chaos-chaos transitions.

In order to detect transitions from quasiperiodic motion to SNAs, we extend this approach to the “white vertical lines” in RPs. Note that these lines represent the time needed by the system to recur to a previously visited state. Here we propose two types of recurrence analysis in order to identify transitions to or from SNAs.

1. Transition from quasiperiodic motion to SNAs: From the RP, we evaluate the frequency distribution  $P^\delta(w)$  of the lengths  $w$  of the white vertical lines. We compute the *mean recurrence time* ( $T_{MRT}$ ) from this distribution,

$$T_{MRT} = \sum_{w=1}^N wP(w) / \sum_{w=1}^N P(w). \quad (2)$$

Furthermore, we determine the *number of recurrence* of the most probable recurrence time ( $N_{MPRT}$ ). It indicates how many times the system has recurred using the most probable recurrence time and is given by

$$N_{MPRT} = \text{Max}(\{P(w)\}; \quad w = 1, \dots, N). \quad (3)$$

We also consider the variance  $\sigma_{MRT}$  of  $T_{MRT}$  and  $\sigma_{MPRT}$  of  $N_{MPRT}$ . For a given sufficiently long trajectory, the variance is evaluated by dividing the trajectory into  $k$  segments and computing  $T_{MRT}$  and  $N_{MPRT}$  for each segment separately. Thus

$$\sigma_{MRT} = \frac{1}{k} \sum_{l=1}^k (T_{MRT}(l) - \overline{T}_{MRT})^2, \quad (4)$$

$$\sigma_{MPRT} = \frac{1}{k} \sum_{l=1}^k (N_{MPRT}(l) - \overline{N}_{MPRT})^2, \quad (5)$$

where the overbar indicates the mean value.

2. Transition from SNAs to chaos: The identification of this transition [40] is based on the *determinism* ( $DET$ ) [32] a measure of complexity defined as the ratio of the sum of all diagonal lines in the RP to the total number of recurrent points.  $DET$  was originally introduced to quantify the predictability of a system: purely deterministic systems are characterized by uninterrupted diagonal lines in the RP. In contrast, the RPs of pure stochastic systems consist mainly of isolated black dots [37]. Since SNAs and chaotic attractors are both fractal, this transition cannot be observed by simply computing the standard  $DET$ ; instead we compute the cross-recurrence plot (CRP) [41] of two time series from two identical systems starting at different initial conditions but driven by the same quasiperiodic force with identical phase. It is now straightforward to detect the transition from SNAs to chaos. If both trajectories synchronize, we obtain an uninterrupted main diagonal line in the CRP. Otherwise, the main diagonal is interrupted. Since trajectories synchronize on SNAs and do not synchronize on chaotic attractors,  $DET$  of the cross-recurrence matrix (CRM)

$$CR_{i,j}^{m,\delta} = (\delta - \|\mathbf{x}_i - \mathbf{y}_j\|), \quad (6)$$

proves to be a useful quantity. In standard notation,  $\mathbf{x}_i$  and  $\mathbf{y}_j$ ,  $i = 1, \dots, N_x$  and  $j = 1, \dots, N_y$ , denote the two separate trajectories and the embedding dimension is  $m$ . As in other computations, we set the delay to 1, and the threshold  $\delta$  is taken in units of the average standard deviation  $\sigma$  of the two time series. From  $DET$  for the main diagonal in the CRP, one can detect the transition from SNAs to chaos.

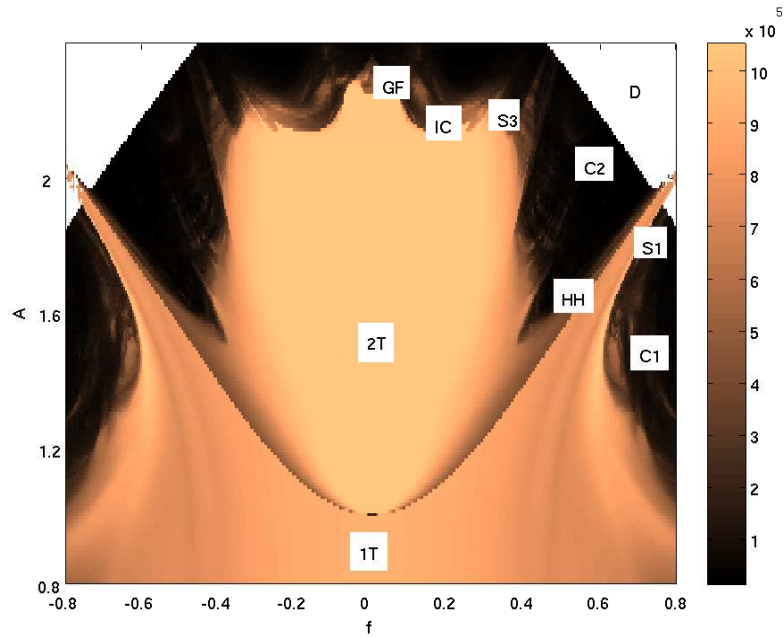


FIG. 1: Phase diagram of the quasiperiodically forced cubic map (Eq.8), obtained using  $N_{MPRT}$  (Eq.3). 1T and 2T correspond to tori of period 1 and 2, respectively. GF correspond to region where the gradual fractalization of the torus occurs. HH represents the region where the SNA is created through the Heagy Hammel route. S1 and S3 denote regions where the SNA appears through Type-I and Type-III intermittencies, respectively. IC denotes the region where SNAs are created through crisis-induced intermittency. C1 and C2 correspond to chaotic regions. For the parameter values in region marked D, the trajectories escape to infinity.

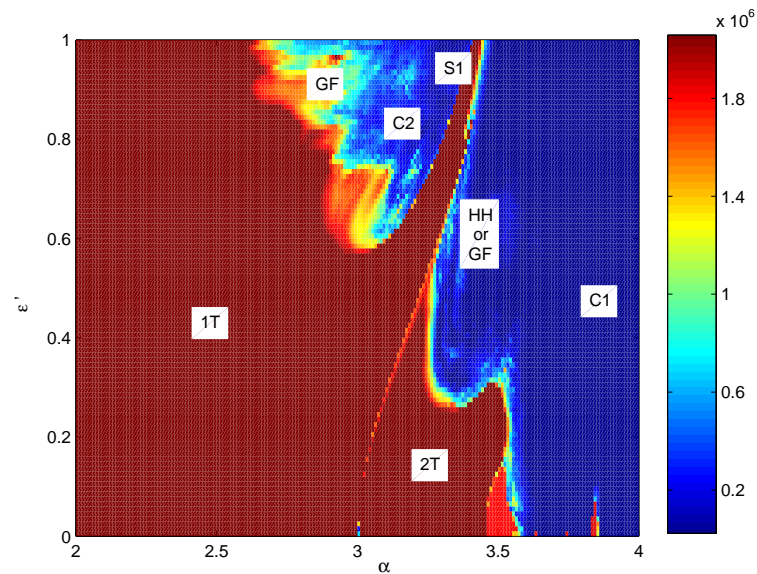


FIG. 2: Phase diagram of the quasiperiodically forced logistic map (Eq.7), obtained using  $N_{MPRT}$  (Eq.3).

### III. THE TRANSITION FROM QUASIPERIODIC DYNAMICS TO SNAS

We study the transition from quasiperiodic dynamics to SNAs in the quasiperiodically forced logistic map

$$\begin{aligned} x_{n+1} &= \alpha[1 + \varepsilon \cos(2\pi\theta_n)]x_n(1 - x_n), \\ \theta_{i+1} &= \theta_i + \omega \bmod 1. \end{aligned} \quad (7)$$

and the quasiperiodically forced cubic map,

$$\begin{aligned}x_{i+1} &= Q + f \cos(2\pi\theta_i) - Ax_i + x_i^3, \\ \theta_{i+1} &= \theta_i + \omega \bmod 1.\end{aligned}\tag{8}$$

These systems have been already investigated and various transitions to SNAs have been identified using tools such as Lyapunov exponents and their variance, as well as finite-time Lyapunov exponents, dimensions, power spectral measures and phase sensitivity exponents [42, 43]. Using  $N_{MPRT}$  (Eq. 3), we obtain first for the logistic and cubic maps two-parameter  $((\varepsilon', \alpha)$  and  $(A, f)$ , respectively) phase diagrams which clearly show changes in the dynamics, that are in strong agreement with those reported in [42, 43]. These phase diagrams were computed using  $\delta = 0.06$  and  $N = 10,000$  normalized data points. The parameter  $\varepsilon' = \varepsilon/(4/\alpha - 1)$  is a rescaled driving parameter.

The phase diagram of the cubic map is given in Fig. 1. It can be observed that the dynamics is symmetric about  $f = 0$ , with two chaotic regions C1 and C2. Bordering these chaotic areas, one finds SNAs which are created through different mechanisms such as Heagy Hammel (HH), gradual fractalization (GF), intermitencies of type-I and type-III (S1, S3) and interior crisis (IC). There are also regions where the dynamics is on quasiperiodic attractors of period 1 and 2 which are marked respectively by 1T and 2T. The phase diagram for the quasiperiodically forced logistic map [43] obtained by using  $N_{MPRT}$ , shown in Fig. 2, exhibits very interesting patterns. Almost all the dynamics found in the phase diagram of the cubic map [42] are also present here.

In order to exemplify the performance of  $T_{MRT}$  and  $N_{MPRT}$ , we analyze in detail two typical transitions to SNAs.

**i) The Heagy Hammel route** in the cubic map (Eq.8). In this route to SNAs, the birth of a SNA is due to the collision between a period-doubled torus with its unstable parent [7]. We fix the bifurcation parameter  $f = 0.7$  and vary  $A$  in the range  $1.8865 \leq A \leq 1.8875$ . At the starting value of  $A$ , we have a period-doubled torus of period 2. As  $A$  increases to the value 1.8868, the torus begins to wrinkle and comes closer and closer to its parent, with which it collides and ultimately gives birth to a fractal attractor when  $A$  is increased up to the value 1.88697. It has been shown that at this value of  $A$ , the attractor possesses a geometrically strange structure and is nonchaotic [42]. Using the threshold  $\delta = 0.001$  and  $N = 10,000$  normalized data points for the computation of the RP, we are able to detect the critical value  $A = 1.88697$  at which both tori collide (Figs. 3a,b). The variances  $\sigma_{MRT}$  and  $\sigma_{MPRT}$ , computed using  $N = 300,000$  data points for the whole trajectory and  $N = 2,000$  data points for each segment, show this transition even more clearly (Figs. 3c,d). One can see that the recurrence time measures vary slightly before the collision and at the critical value there is a drastic jump, after which, some oscillations start indicating an irregular behavior.

**ii) The Intermittency route** wherein a strange attractor disappears and is replaced by a one-frequency torus through an analog of the saddle-node bifurcation. In the vicinity of this phenomenon the attractor is strange and nonchaotic. It has been shown that the dynamics at this transition is intermittent, and the scaling behavior is characteristic of Type-I intermittency [13, 44]. In the logistic map, this intermittency route to SNAs (denoted S1) occurs along the right edge of the chaotic region C2 in Fig. 2. For  $\varepsilon' = 1$  and varying  $\alpha$ , we see in Fig. 4 that the measures fluctuate rather strongly in the SNA regime and smoothly in the quasiperiodic one. There is an abrupt change at the critical value  $\alpha_c \approx 3.4058088$  where the intermittent transition takes place. The threshold is set to  $\delta = 0.03$ . For the computation we have used  $N = 10,000$  normalized data points for  $N_{MPRT}$  and  $T_{MRT}$ ,  $N = 300,000$  for the variances and  $N = 2,000$  as length of each segment.

We have also identified other routes to SNAs by these measures. Indeed, all four measures based on RPs are able to detect these transitions. Since the mechanism for the creation of SNAs is different for each route, it was not easy to find a satisfactory threshold for the computation of the RP which holds for all the different routes to SNAs. However, for each route to SNAs, we are able to find a threshold which lead to a good detection of the transition to SNAs by the recurrence time measures.

The robustness of the measures against noise has also been investigated. It is known that noise generally decreases the threshold for chaos since transitions and bifurcations get blurred in the presence of fluctuations. For added noise in the case of the HH route in the cubic map (Eq.8), our results are shown in Figs. 5a,c show  $T_{MRT}$  and  $N_{MPRT}$ . Uniformly distributed noise of amplitude  $10^{-4}$  has been added to the variable  $x$  (in order to keep the quasiperiodicity of the forcing). Figs. 5b,d represent the case of uniformly distributed noise of amplitude 0.01. The transition from torus to SNAs globally survives. In the case of dynamical noise and especially for  $T_{MRT}$  (Fig. 5a), noise has considerably reduced the value of the bifurcation parameter at which the transition to SNAs appears, but the recurrence time measures are still able to detect the transition.

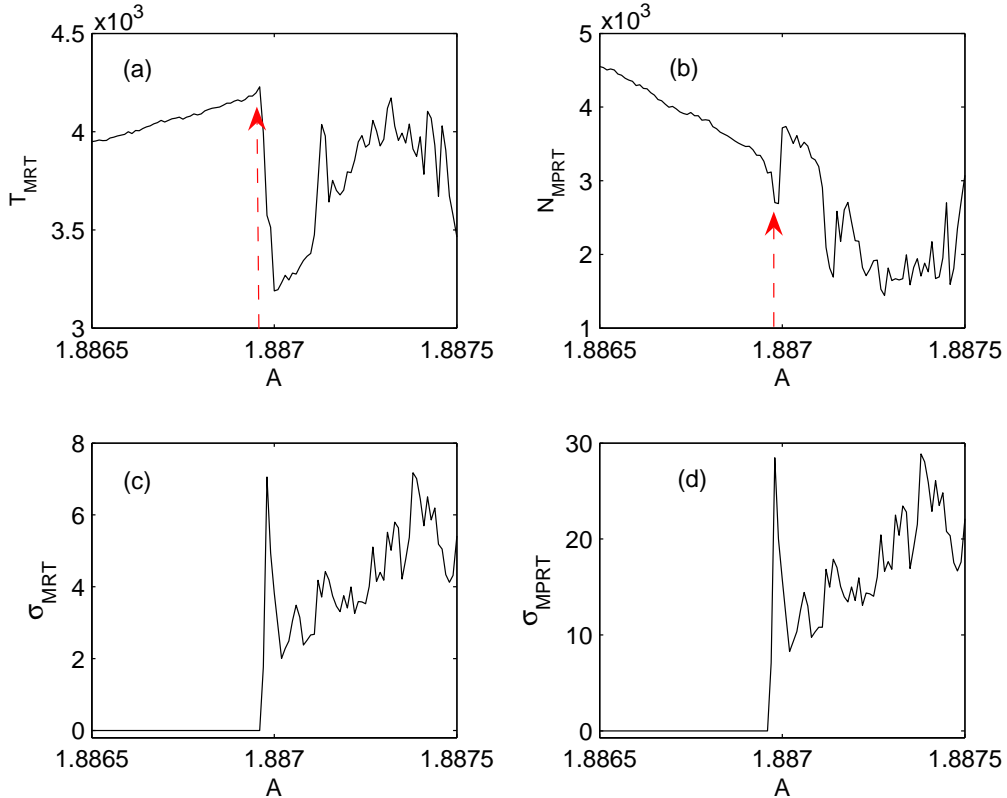


FIG. 3: Transition from doubled torus to SNA through HH mechanism in the cubic map (Eq.8). (a): Behavior of  $T_{MRT}$ ; (b): Behavior of  $N_{MPRT}$ ; (c): Variance of  $T_{MRT}$ ; (d): Variance of  $N_{MPRT}$ . The critical value is  $A \approx 1.88697$ .

#### IV. FRACTALIZATION ROUTE TO SNA

The fractalization of a torus is both the most common and the most intriguing transition to SNAs. In this mechanism, a torus becomes more and more wrinkled as the forcing increases until it breaks up to form a strange set. The fractalization appears as a gradual change in the structure of the attractor which is difficult to relate to a precise bifurcation point, where a sudden change in the dynamics occurs due to the crossing of a well-defined critical threshold. In some particular cases, namely for forced noninvertible maps, it is possible to define a critical threshold for the fractalization transition. In contrast to other mechanisms for the emergence of SNAs, there is no obvious unstable set involved in the fractalization route. Datta *et al.* [46] have however recently used techniques introduced by Kim *et al.* [47] to find unstable sets for the fractalization process using a sequence of rational approximations of the irrational forcing. They found that these unstable sets are created through a cascade of period-doubling bifurcations, and collision of chaotic bands with them causing a cascade of interior merging crises whereby the fractalization process takes place.

The first example we study is the fractalization route in the forced logistic map as described by Nishikawa and Kaneko [12]:

$$\begin{aligned} x_{n+1} &= ax_n(1-x_n) + \varepsilon \sin(2\pi\theta_n), \\ \theta_{n+1} &= \theta_n + \omega \text{ mod } 1. \end{aligned} \quad (9)$$

We fix  $a = 3$  and vary  $\varepsilon$ . At  $\varepsilon = 0$ , the attractor of the system is a straight-line torus. As  $\varepsilon$  is increased, oscillations of the torus start to appear and it becomes fractal at  $\varepsilon \approx 0.1553$ . The variances  $\sigma_{MRT}$  and  $\sigma_{MPRT}$  vary slightly but at the critical value  $\varepsilon_c \approx 0.1553$ , they suddenly increase and their fluctuations become larger for the following values of the bifurcation parameter (Fig. 6). As  $\varepsilon$  is increased further, a transition from the fractal torus to chaos takes place at  $\varepsilon \approx 0.1573$ .

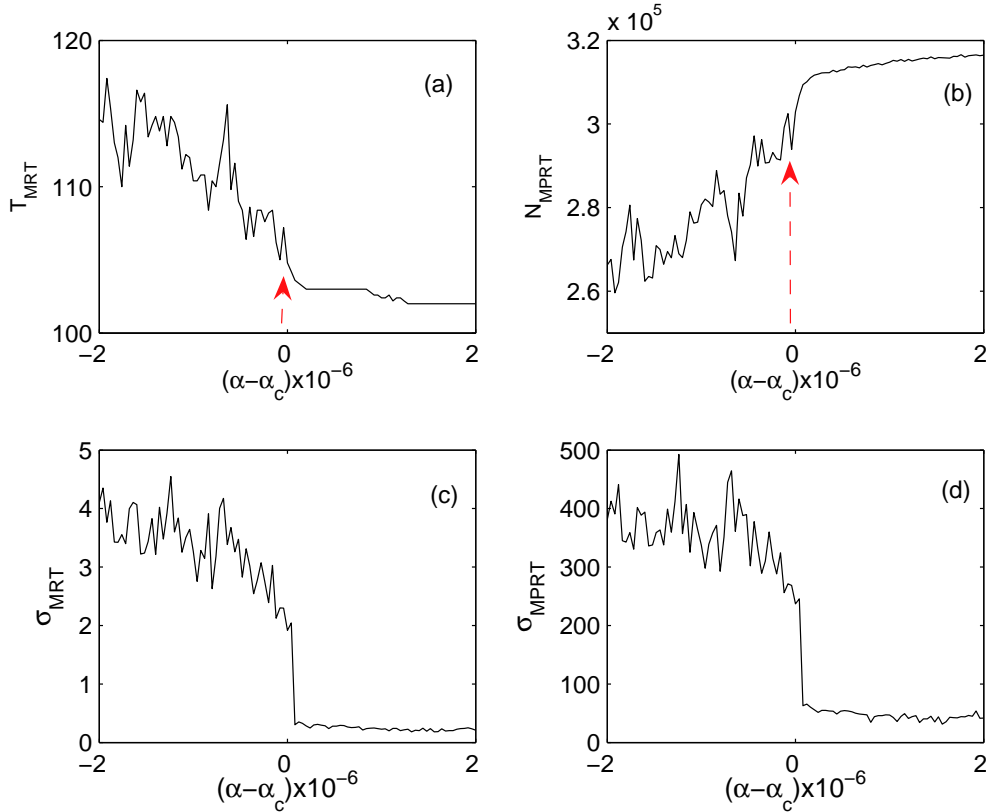


FIG. 4: Type-I intermittency route in the logistic map (Eq.7). (a): Behavior of  $T_{MRT}$ ; (b): Behavior of  $N_{MPRT}$ ; (c): Variance of  $T_{MRT}$ ; (d): Variance of  $N_{MPRT}$ . The critical value is  $\alpha_c \approx 3.4058088$ .

A second example that we consider is the fractalization route in the Hénon map [45], given by the equations

$$\begin{aligned} u_{n+1} &= 1 + v_n - bu_n^2 + A\cos(2\pi\theta_n), \\ u_{n+1} &= cu_n, \\ \theta_{n+1} &= \theta_n + \omega \text{ mod } 1, \end{aligned} \quad (10)$$

with  $c = 0.1$  and  $A = 0.7$ . The bifurcation parameter is  $b$ . Sosnovtseva *et al.* [45] have found that the transition to SNAs happens at  $b = 0.7$ ; strange nonchaotic behavior is then replaced by a chaotic behavior as  $b$  is increased to the value  $b = 0.77$ . We find the transition closer to 0.69 when there is an abrupt increase in  $\sigma_{MRT}$  and  $\sigma_{MPRT}$ ; see Fig. (7).

## V. THE TRANSITION FROM SNAS TO CHAOTIC ATTRACTORS

The transition from SNAs to chaotic attractors is a purely dynamical one: the structure of the attractor remains essentially unchanged, while the largest Lyapunov exponent becomes positive. This is a consequence of the manner in which the invariant measure is redistributed on the attractor [48]. Since the largest Lyapunov exponent of SNAs is negative, two such systems are able to undergo complete synchronization. It has been shown in [22] that regardless of the initial conditions of two identical SNAs, they eventually converge to the same dynamics if the phase of the quasiperiodic driving coincides for both of them. In contrast, in the chaotic regime, both systems have positive Lyapunov exponents, and therefore, they cannot synchronize. A recurrence measure, which can easily identify the synchronization, and hence the transition from SNAs to chaos, is based on the  $DET$  of the CRM defined in Eq. (6) for two different time series generated by the same initial phase  $\theta_0$ . If both trajectories synchronize, we obtain an

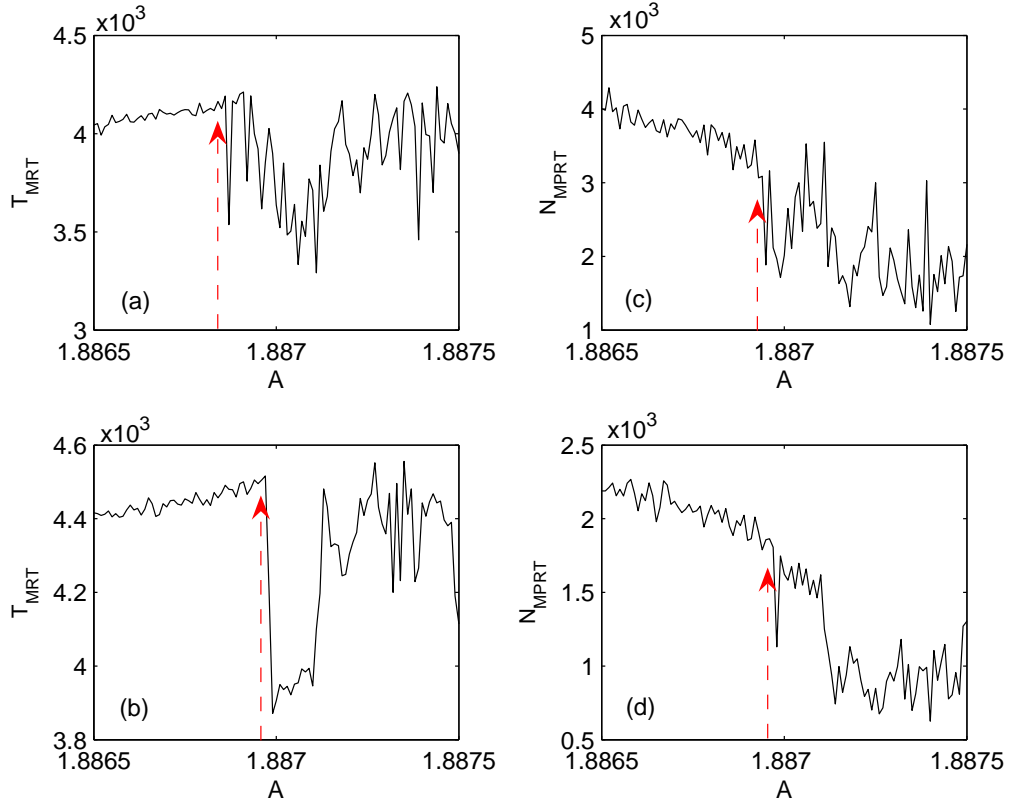


FIG. 5: Robustness of the recurrence time measures against noise for HH route in the cubic map(Eq.8). (a) and (c):  $T_{MRT}$  and  $N_{MPRT}$  for dynamical noise of amplitude  $10^{-4}$ ; (c) and (d):  $T_{MRT}$  and  $N_{MPRT}$  for observational noise of amplitude 0.01. Threshold used  $\delta = 0.001$  and  $N = 10,000$  normalized data points.

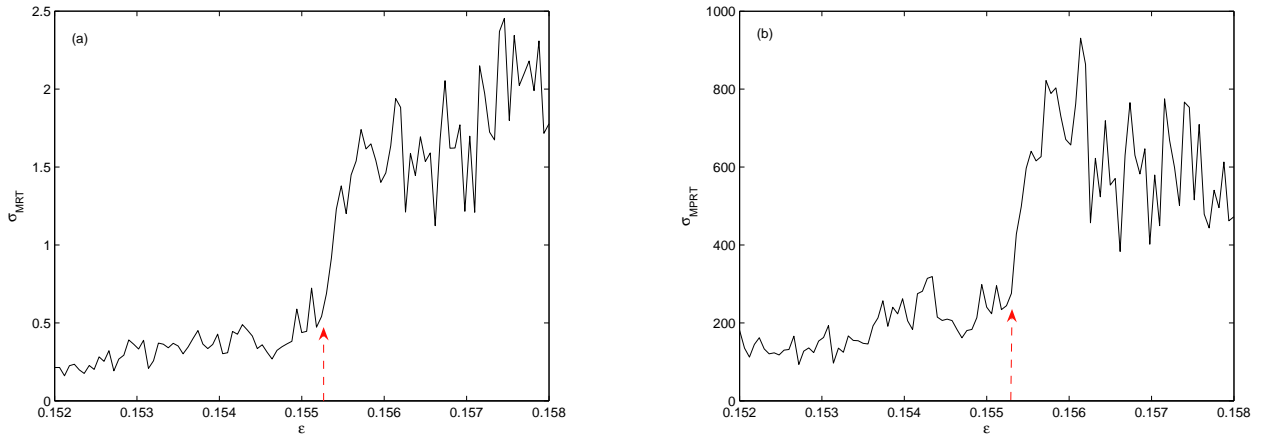


FIG. 6: Fractalization route in the logistic map(Eq.9). (a): Variance of  $T_{MRT}$ ; (b): Variance of  $N_{MPRT}$ ; Variances computed using  $\delta = 0.05$ ,  $N = 750,000$  data points as the whole trajectory and  $N = 3,000$  as length of each segment. The critical value of bifurcation parameter is  $\epsilon_c \approx 0.1553$ .

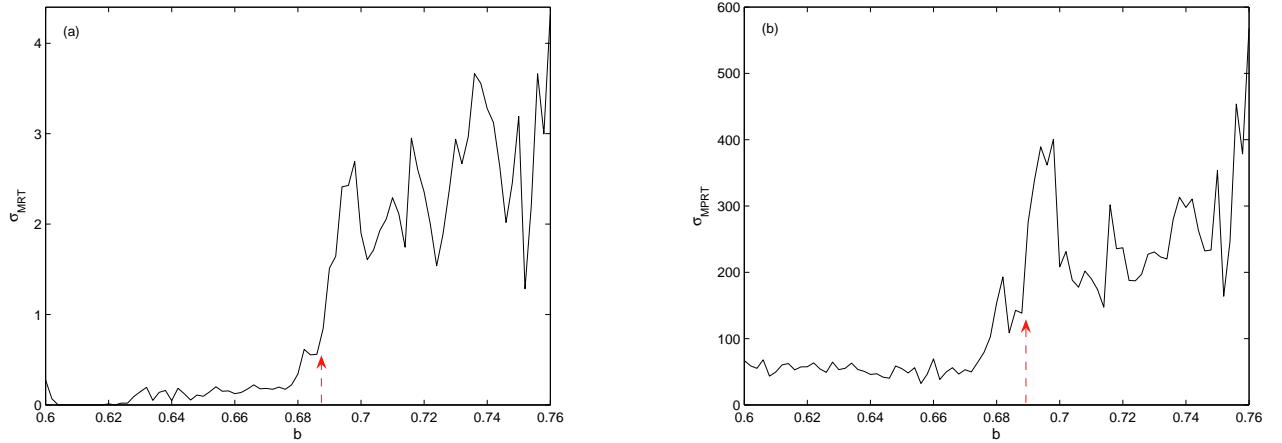


FIG. 7: Fractalization route in the Hénon map (Eq.10). (a): Variance of  $T_{MRT}$ ; (b): Variance of  $N_{MPRT}$ . Variances computed using  $\delta = 0.05$ , 750,000 data points and 2,500 as length of each segment. The variances increase suddenly at bifurcation parameter  $b \approx 0.69$ .

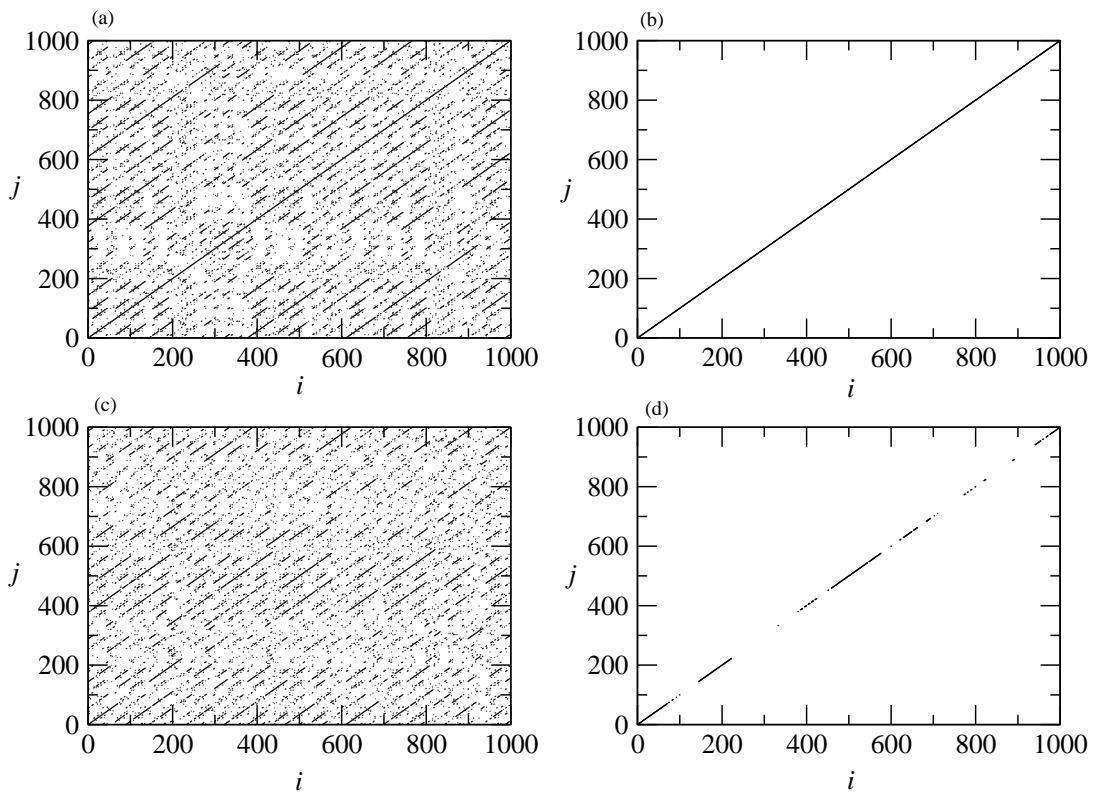


FIG. 8: CRP of the forced logistic map (Eq.7): (a) in the SNA regime with  $\alpha = 3.32$ ,  $\varepsilon' = 0.595$ , and (c) in the chaotic regime with  $\alpha = 3.33$ ,  $\varepsilon' = 0.595$ . Due to synchronization, the CRP and the ordinary RP are identical in the SNA regime, whereas this is not so in the chaotic one. In (b) and (d) only the main diagonals for the SNAs and chaotic attractors are shown. The threshold for the computation of the CRP is  $\delta = 0.2\sigma$  and the embedding dimension is  $m = 3$ .

uninterrupted main diagonal in the CRP. Otherwise, the main diagonal is interrupted indicating that we are in the chaotic regime. This can be clearly seen in Fig. 8 where the CRPs are illustrated for both cases. Thus, by computing the  $DET$  of the CRP only on the main diagonal, the transition from SNAs to chaos can be detected very clearly. In

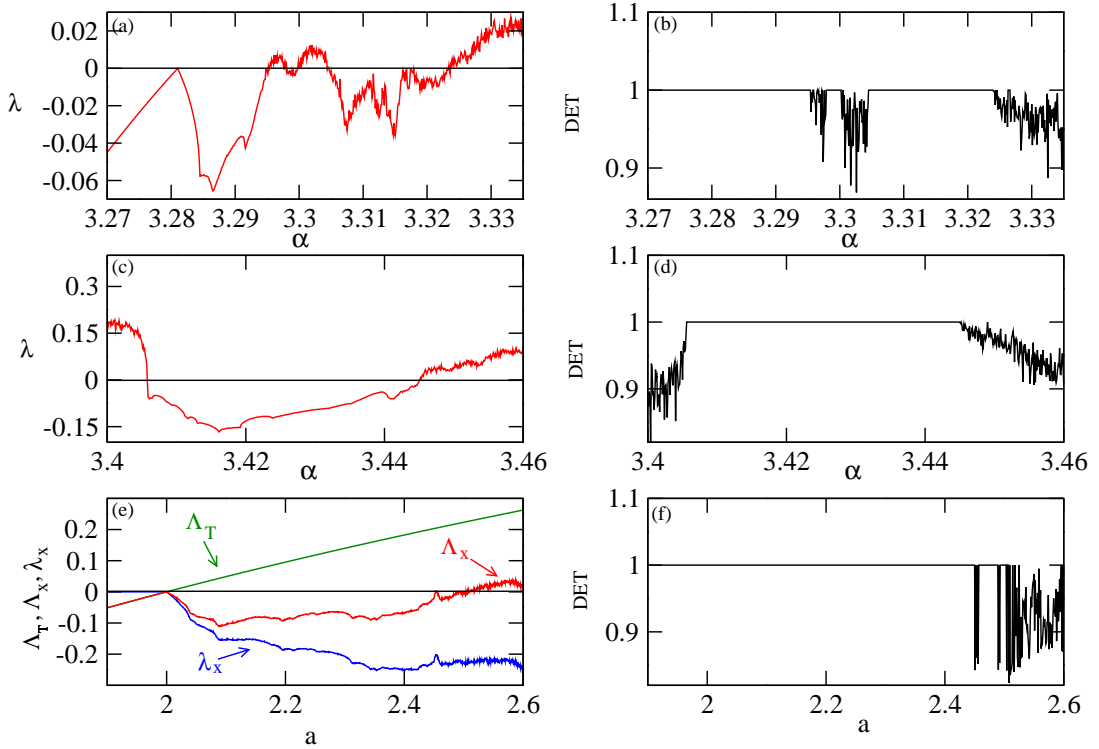


FIG. 9: Comparison of the Lyapunov exponent ( $\lambda$ ) and  $DET$  for the CRPs on the main diagonal line. (a)  $\lambda$  for Eq. 7 with  $\varepsilon' = 0.595$ , (b) the corresponding  $DET$ , (c)  $\lambda$  for Eq. 7 with  $\varepsilon' = 1$ , (d) the corresponding  $DET$ , (e)  $\Lambda_T$ ,  $\Lambda_x$  and  $\lambda_x$  for Eq. 11 and (f) the corresponding  $DET$ . A  $DET$  value of unity corresponds to SNAs dynamics, and a drop in the value of  $DET$  to lower values indicates the SNAs to chaos transition. In all cases studied here, we use  $\delta = 0.2\sigma$  and embedding dimension is  $m = 3$ .

the SNAs regime  $DET = 1$ , while in the chaotic regime  $DET < 1$ .

The specific characteristics of SNAs depend on the mechanisms through which they were created, and it appears that this feature carries over into the corresponding chaotic attractors. Accordingly, we have numerically examined the SNAs to chaos transition for SNAs created via the HH [7] and intermittency [13] routes in the quasiperiodically forced logistic map (Eq. 7). We have also studied the mapping

$$\begin{aligned} x_{n+1} &= (a \cos 2\pi\theta_n + b) \sin 2\pi x_n, \\ \theta_{n+1} &= \theta_n + \omega \text{ mod } 1. \end{aligned} \quad (11)$$

where the blowout bifurcation [24] route to SNAs has been observed.

These results are shown in Fig. 9. For the HH route we use  $\varepsilon' = 0.595$  (see Fig.2) in the logistic map. Figs. 9(a,b) show the Lyapunov exponent and the  $DET$  respectively. As it can be clearly seen, when the Lyapunov exponent changes from negative to positive, this is accompanied by a sharp drop in the value of  $DET$ . Analogously, for the intermittency route to chaos at  $\varepsilon' = 1$ , the behaviour of the Lyapunov exponent and  $DET$  are shown in Figs. 9(c,d).

For the transition along the blowout bifurcation route, the nontrivial Lyapunov exponent  $\Lambda_x$  is compared to  $DET$  and shows the SNAs to chaos transition; see Figs. 9(e,f).  $\Lambda_x$  is deduced from the transverse Lyapunov exponent  $\Lambda_T$  via [24]

$$\Lambda_x = \Lambda_T - |\lambda_x|, \quad (12)$$

where  $\lambda_x$  is the nonzero Lyapunov exponent of Eq. (11).

The measure showing the transition from SNAs to chaos is found to be robust to added external noise. This is very important in context to analysis of experimental data. In Fig. 10, we show the effect of uniform additive noise, in Eq. 7 for the HH and the intermittency routes.

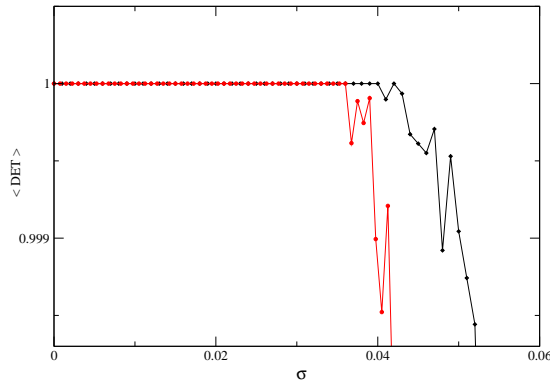


FIG. 10:  $DET$  (averaged over 200 stochastic runs) for Eq. 7 with increasing noise amplitude  $\sigma$ . The line with diamonds corresponds to the HH route at  $\alpha = 3.32$  and  $\varepsilon' = 0.595$ . The line with filled circles corresponds to the intermittency route at  $\alpha = 3.385$  and  $\varepsilon' = 0.8$ . We use  $\delta = 0.2\sigma$  and the embedding dimension is  $m = 3$ .

## VI. SUMMARY

Our main objective in this work has been to use recurrence time statistics in order to detect transitions to or from SNAs. To detect the transition from quasiperiodic motion to SNAs, we have introduced four measures, namely  $T_{MRT}$ ,  $N_{MPRT}$  and their variances, which are based on the time needed by the system to recur to a neighborhood of a previous point of the trajectory. These measures have been able to detect the onset of the strange nonchaotic dynamic in the Heagy–Hammel and intermittency routes respectively in the cubic and logistic maps. Moreover, they also detect the fractalization of a torus to SNAs. We have seen for example in the Heagy–Hammel route that these four measures vary slightly in the quasiperiodic regime. At the critical value of the bifurcation parameter, there is a drastic jump followed by irregular fluctuations of the recurrence time measures indicating the SNA regime.

The transition from SNAs to chaos has also been identified by computing the determinism for a cross-recurrence plot of two different time-series generated by the same initial phase. At the critical value, we have noticed a sharp change in the value of the determinism from its maximum value 1.

These measures—which are robust against noise—can detect these transitions even when the orbits are not very long, in contrast to Lyapunov exponent based measures. The present measures are also advantageous in the sense that they do not require the knowledge of the equations governing the system under study. Therefore, they are suitable for the analysis of experimental data. Illustrations of the applicability of these measures for continuous systems and experimental data will be provided in a separate paper.

**Acknowledgment:** This work was supported by the Deutscher Akademischer Austausch Dienst (EJ), the Promotion Kolleg (EJ, MC, JK) and SPP1114 (MT, JK). AN is supported by the CSIR, India. We thank Awadhesh Prasad and Dr. N. Marwan for very helpful suggestions and discussions.

- 
- [1] L. D. Landau, Dokl. Akad. Nauk SSSR **44**, 339 (1944).
  - [2] D. Ruelle and F. Takens, Comm. Math. Phys. **20**, 167 (1971).
  - [3] C. Grebogi, E. Ott, S. Pelikan and J. A. Yorke, Physica D **13**, 261 (1984).
  - [4] A. Bondeson, E. Ott and T. M. Antonsen, Phys. Rev. Lett. **55**, 2103 (1985).
  - [5] F. J. Romeiras and E. Ott, Phys. Rev. A **35**, 4404 (1987).
  - [6] M. Ding, C. Grebogi and E. Ott, Phys. Rev. A **39**, 2593 (1989).
  - [7] J. F. Heagy and S. M. Hammel, Physica D **70**, 140 (1994).
  - [8] A. Pikovsky and U. Feudel, Chaos **5**, 253 (1995).
  - [9] U. Feudel, J. Kurths and A. Pikovsky, Physica D **88**, 176 (1995).
  - [10] M. Ding and J. Scott Kelso, Int. J. Bifurcation Chaos Appl. Sci. Eng. **4**, 553 (1994).
  - [11] Y.-C. Lai, Phys. Rev. E **53**, 57 (1996).
  - [12] T. Nishikawa and K. Kaneko, Phys. Rev. E **54**, 6114 (1996).
  - [13] A. Prasad, V. Mehra and R. Ramaswamy, Phys. Rev. Lett. **79**, 4127 (1997).

- [14] A. Venkatesan and M. Laksmanan, Phys. Rev. E **58**, 3008 (1998).
- [15] W. L. Ditto et al, Phys. Rev. Lett. **65**, 553 (1990).
- [16] T. Zhou, F. Moss and A. Bulsara, Phys. Rev. A **45**, 5394 (1992).
- [17] G. Keller, Fundamenta Mathematicae **151**, 139 (1996).
- [18] J. Stark, Physica D **109**, 163 (1997).
- [19] R. Sturman and J. Stark, Nonlinearity **13**, 113 (2000).
- [20] B. R. Hunt and E. Ott, Phys. Rev. Lett. **87**, 254101 (2001).
- [21] A. Prasad, B. Biswal and R. Ramaswamy, Phys. Rev. E **68**, 037201 (2003).
- [22] R. Ramaswamy, Phys. Rev. E **56**, 7294 (1997).
- [23] C.-S. Zhou and T.-L. Chen, Europhys. Lett. **38**, 261 (1997).
- [24] T. Yalçinkaya and Y.-C. Lai, Phys. Rev. Lett. **77**, 5039 (1996).
- [25] T. Kapitaniak and J. Wojewoda, *Attractors of Quasiperiodically Forced Systems*, (World Scientific, Singapore, 1993).
- [26] V. S. Anishchenko, T. K. Vadivasova and O. Sosnovtseva, Phys. Rev. E **53**, 4451 (1996).
- [27] U. Feudel, S. Kuznetsov and A. Pikovsky, *World Scientific Series on Nonlinear Science*, Series A, Vol. 56.
- [28] K. Thamilmaran, D. V. Senthilkumar, A. Venkatesan and M. Lakshmanan Phys. Rev. E **74**, 036205 (2006).
- [29] H. Poincaré, Acta Math. **13**, 1 (1890).
- [30] J. P. Eckmann, S. O. Kamphorst and D. Ruelle, Europhys. Lett. **4**, 973 (1987).
- [31] G. M. Mindlin and R. Gilmore, Physica D **581**, 229 (1992).
- [32] J. P. Zbilut and J. R. Webber, Phys. Lett. A **171**, 199 (1992).
- [33] M. Thiel et al, Physica D **171**, 138 (2002).
- [34] C. L. Weber Jr. and J. P. Zbilut, Journal of Applied Physiology **76(2)**, 965 (1994).
- [35] K. Shockley, M. Butwill, J. P. Zbilut and C. L. Webber Jr., Phys. Lett. A **59**, 305 (2002).
- [36] N. Marwan, M. Thiel, and N. R. Nowaczyk, Nonlinear Processes in Geophysics **9 (314)**, 325 (2002).
- [37] N. Marwan, M. C. Romano, M. Thiel and J. Kurths, *Recurrence Plots for the Analysis of Complex Systems*, Physics Reports (in press).
- [38] J. B. Gao, Phys. Rev. Lett. **83**, 3178 (1999).
- [39] N. Marwan, N. Wessel, U. Meyerfeldt, A. Schirdewan and J. Kurths, Phys. Rev. E **66**, 026702 (2002).
- [40] Y.C. Lai, Phys. Rev. E **53**, 57 (1996).
- [41] N. Marwan and J. Kurths, Phys. Lett. A **302**, 299 (2002).
- [42] A. Venkatesan and M. Laksmanan, Phys. Rev. E **63**, 026219 (2001).
- [43] A. Prasad, V. Mehra and R. Ramaswamy, Phys. Rev. E **57**, 1576 (1998).
- [44] Y. Pomeau and P. Manneville, Comm. Math. Phys. **74**, 189 (1980).
- [45] O. Sosnovtseva, U. Feudel, J. Kurths and A. Pikovsky, Phys. Lett. A **218**, 255 (1996).
- [46] S. Datta, R. Ramaswamy and A. Prasad Phys. Rev. E **70**, 046203 (2004).
- [47] S.-Y. Kim, W. Lim and E. Ott Phys. Rev. E **67**, 056203 (2003).
- [48] S. S. Negi, A. Prasad and R. Ramaswamy, Physica D **145**, 1 (2000).